Molecular Crystals and Liquid Crystals
Publication details, including instructions for authors and subscription information:
http://www.tandfonline.com/loi/gmcl16

Dilatometric and Thermobarometric Measurements of Truxene Derivatives Exhibiting Inverted and Reentrant Sequences

J. M. Buisine [a] , R. Cayuela [b] , C. Destrade [b] & Nguyen Huu Tinh [b]

[a] Equipe de Dynamique des Cristaux Moléculaires, U.A. C.N.R.S. 801, Université des Sciences et Techniques de Lille Flandres Artois, 59655, Villeneuve d'Ascq, Cédex, FRANCE

[b] Centre de Recherche Paul Pascal, Domaine Universitaire, 33405, Talence, Cédex, FRANCE

Version of record first published: 21 Mar 2007.

To cite this article: J. M. Buisine , R. Cayuela , C. Destrade & Nguyen Huu Tinh (1987): Dilatometric and Thermobarometric Measurements of Truxene Derivatives Exhibiting Inverted and Reentrant Sequences, Molecular Crystals and Liquid Crystals, 144:5, 137-160

To link to this article: http://dx.doi.org/10.1080/15421408708084210

Mol. Cryst. Liq. Cryst., 1987, Vol. 144, pp. 137–160
Photocopying permitted by license only

Printed in the United States of America

Dilatometric and Thermobarometric Measurements of Truxene Derivatives Exhibiting Inverted and Reentrant Sequences

J. M. BUISINE

Equipe de Dynamique des Cristaux Moléculaires, U.A. C.N.R.S. 801, Université des Sciences et Techniques de Lille Flandres Artois, 59655 Villeneuve d'Ascq Cédex-FRANCE

and

R. CAYUELA, C. DESTRADE and NGUYEN HUU TINH

Centre de Recherche Paul Pascal, Domaine Universitaire, 33405 Talence Cédex-FRANCE

(*Received October 3, 1986*)

Members of the truxene derivatives series Cn HATX have been investigated by density-temperature—for n = 8 to 12—and thermobarometric—for n = 8, 10 to 13—measurements. Volume changes for transitions, density, partial molar volumes for aromatic cores and CH_2 groups, thermal expansion and isothermal compressibility coefficients are determined for the discoid nematic N_D and rectangular columnar D_{rd} mesophases. Pressure-temperature phase diagrams for n = 8, 10 to 13 are given; a monotropic phase is observed under atmospheric pressure for n = 10 and 11; it seems it is an hexagonal columnar mesophase D_h. Maximum for the boundary line for D_h and N_D or D_{rd} phases for n = 10 and 12 are predicted.

Keywords: disc-like mesogens, reentrant sequences, density, molar volume, P-T phase diagram

INTRODUCTION

For disc-like mesogens, although some data relating to the molar volume-temperature dependence for mesophases,[1] volume changes and pressure-temperature dependence for the transitions[1–5] are known for normal sequences, such data do not exist for inverted[6–7] or reentrant[8–10] sequences. We report here dilatometric and thermobarometric measurements of truxene derivatives exhibiting both inverted and reentrant sequences.[11]

I. SUBSTANCES

The studied compounds are members of the hexa-alkanoyloxy truxene homologous series (Cn HATX):[11]

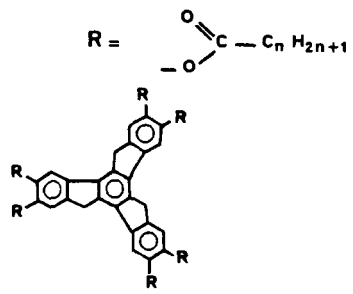

For the short chain derivatives (n = 6 to 11), inverted sequences appear under atmospheric pressure:

$$K \quad [N_D] \quad D_{rd} \quad D_h \quad I \qquad (n = 6 \text{ to } 8),$$

$$K \quad N_D \quad D_{rd} \quad D_h \quad I \qquad (n = 9 \text{ to } 11).$$

For longer chain lengths (n = 12 to 15) a monotropic hexagonal columnar phase appear under atmospheric pressure:

$$K \quad [D_h] \quad N_D \quad D_{rd} \quad D_h \quad I.$$

Experiments have been performed for dilatometric measurements on derivatives with n = 8 to 12, for thermobarometric measurements on derivatives with n = 8, 10 to 13. For all the studied compounds, literature data for the transitions temperatures and enthalpy changes are reported in Table I.

II. DENSITY ANALYSIS

The dilatometric studies have been performed with a commercial electronic densitometer (PAAR-DMA 602 MH) allowing density versus temperature measurements for fluid phases. The apparatus was scaled with standard fluids for which the density versus temperature is known with a good accuracy: styrene and nonane (maximum tem-

TABLE I

Literature and experimental data for the transitions of C_n HATX:

T: Transition temperature (°C),

$\Delta\mathcal{H}$: Enthalpy change (kcal·mole^{-1}),

$\left(\frac{dP}{dT}\right)^E$: Slope of the equilibrium curves (bar·K^{-1}),

$\Delta\mathcal{V}$: Volume change (cm^3·mole^{-1}),

(i) dilatometric and (ii) thermobarometric measurements.

		K_3	K_2	K_1	D_h	N_D	D_{rd}	D_h	ref
$n = 8$	T	—	—	. 88	—	. [87]	. 141	.	11
	$\Delta\mathcal{H}$			7.6		0.3	≃ 0	11	
	$\left(\frac{dP}{dT}\right)^E$			20.9		22.2			
	$\Delta\mathcal{V}^{(i)}$					2.3			
	$\Delta\mathcal{V}^{(ii)}$			42.2		1.6			
$n = 9$	T	—	—	. 68	—	. 85	. 138	.	11
	$\Delta\mathcal{H}$			5.1		] 0.24	≃ 0		11
	$\Delta\mathcal{V}^{(i)}$					1.3			
$n = 10$	T	—	—	. 62	—	. 89	. 118	.	11
	$T^{(ii)}$			. 61.8	. [56]	.			
	$\Delta\mathcal{H}$			8.4		0.21	≃ 0		11
	$\left(\frac{dP}{dT}\right)^E$			26.9	17	26	175		
	$\Delta\mathcal{V}^{(i)}$					1.5			
	$\Delta\mathcal{V}^{(ii)}$			38.8		0.93			
$n = 11$	T	—	—	. 64	—	. 83.5	. 130	.	11
	$T^{(ii)}$			. 65	. [58.5]	.			
	$\Delta\mathcal{H}$			15.7		0.2	≃ 0		11
	$\left(\frac{dP}{dT}\right)^E$			25	14	18			
	$\Delta\mathcal{V}^{(i)}$					2.1			
	$\Delta\mathcal{V}^{(ii)}$			77.7		1.3			
$n = 12$	T	—	—	. 57	. [53]	. 85	. 112	.	11
	$T^{(ii)}$	. 50	. 78	. [56]		.			
	$\Delta\mathcal{H}$			8.2		0.24			
	$\left(\frac{dP}{dT}\right)^E$	34	25.5	29	20	23.5	72.7		
	$\Delta\mathcal{V}^{(i)}$					undefinable	≃ 0		
	$\Delta\mathcal{V}^{(ii)}$			35.8		1.19			
$n = 13$	T	—	—	. 61	. [56]	. 84	. 112	.	11
	$T^{(ii)}$		. 82	. [61]		.			
	$\Delta\mathcal{H}$			20.4		0.1	≃ 0		11
	$\left(\frac{dP}{dT}\right)^E$		20.9	23	13	22			
	$\Delta\mathcal{V}^{(ii)}$			111		0.53			

perature for the calibration: 120°C). More, compounds progressively decompose when they are heated during a long time at high temperature, so only a few number of experiments have been performed on each side of the transition on heating. The monotropic [D_h] phase for $n = 12$ has not been studied because on cooling the crystallization can suddenly appear and can destroy the measurement cell. The volume of the samples is about .1 ml.

Figure 1 (a to f) gives experimental results for density measurements versus temperature for the studied compounds. For $n = 8$ to 11, at the N_D-D_{rd} transition, it occurs important changes for the density. Because of the few number of measurements, it is not possible to determine separately at the transformation, the pretransitional effects[12-13] and the transition. However middle values for the volume changes $\Delta\mathcal{V}$ can be determined; they are reported in Table I.

For $n = 12$ (Figure 1e) although anomalies appear for the density near the transition temperature (detected by optical microscopy) no volume change can be determined; it seems the pretransitional effects conceal the detection of the transition. At the D_{rd}-D_h transformation (Figure 1f) only a change of slope appears at 109°C (transition with no apparent volume change).

Out of transitions, changes for the density versus temperature can be described by the relation $\rho(T) = a - bT$. Data for the coefficients a and b are reported in Table II. For $n = 8$ to 11, expansion coefficients α versus temperature are plotted Figure 2 (a to d). The N_D-D_{rd} transitions are clearly detectable by a divergence for α. For all the studied compounds, middle values for α at a given temperature are reported in Table II. The α variations versus the carbon number of the alkyl chains are weak. The larger data for α in D_h phase (very organized mesophase) than in N_D phase can be explained by the higher temperature for the D_h existence domain.

III. THERMOBAROMETRIC ANALYSIS

The thermobarometric measurements have been performed with an automatic metabolemeter.[14] Details relative to the method, interpretation and exploitation of thermobarograms are given elsewhere.[15-17] The volume of the studied samples is about .002 ml.

Figure 3 gives thermobarograms obtained on heating (a) and on cooling (b) for $n = 8$. Under pressure N_D is always observed as a monotropic phase. Two thermobarograms for $n = 10$ are given Figure 4 on heating (a) and cooling (b). Figure 4b shows the N_D-D_{rd} tran-

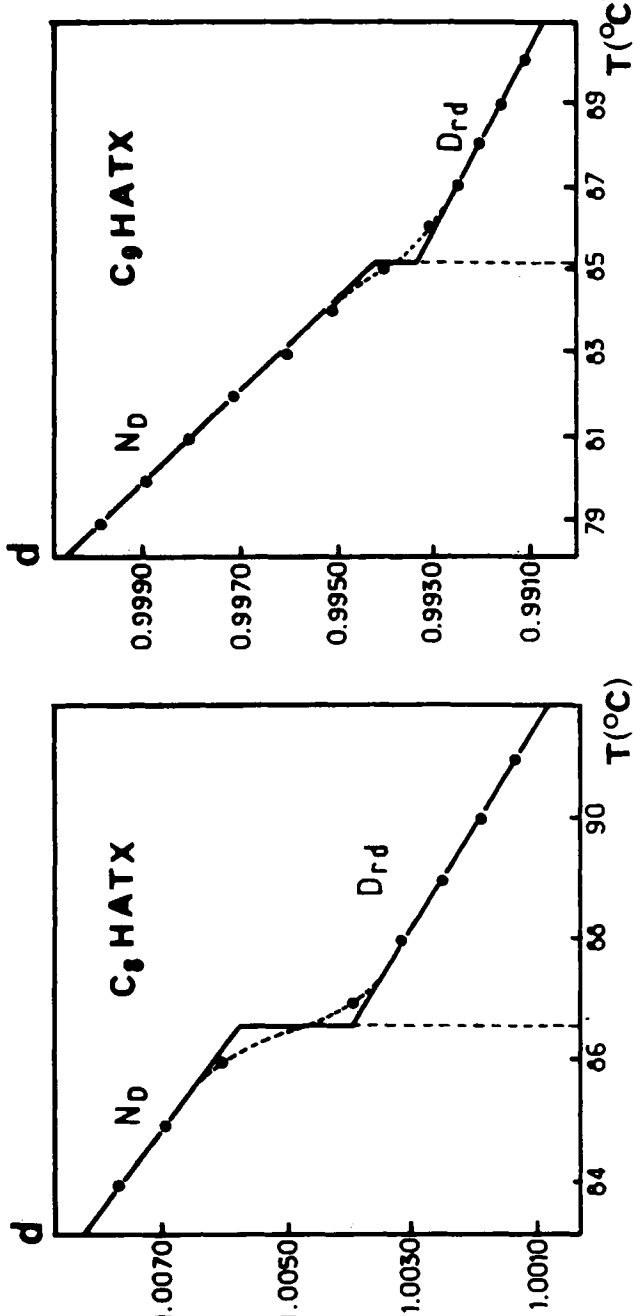

FIGURE 1 Density versus temperature for Cn HATX near the N_D-D_{rd} transition; (a): $n = 8$, (b): $n = 9$, (c): $n = 10$, (d): $n = 11$, (e): $n = 12$ and near the D_{rd}-D_h transition (f): $n = 12$.

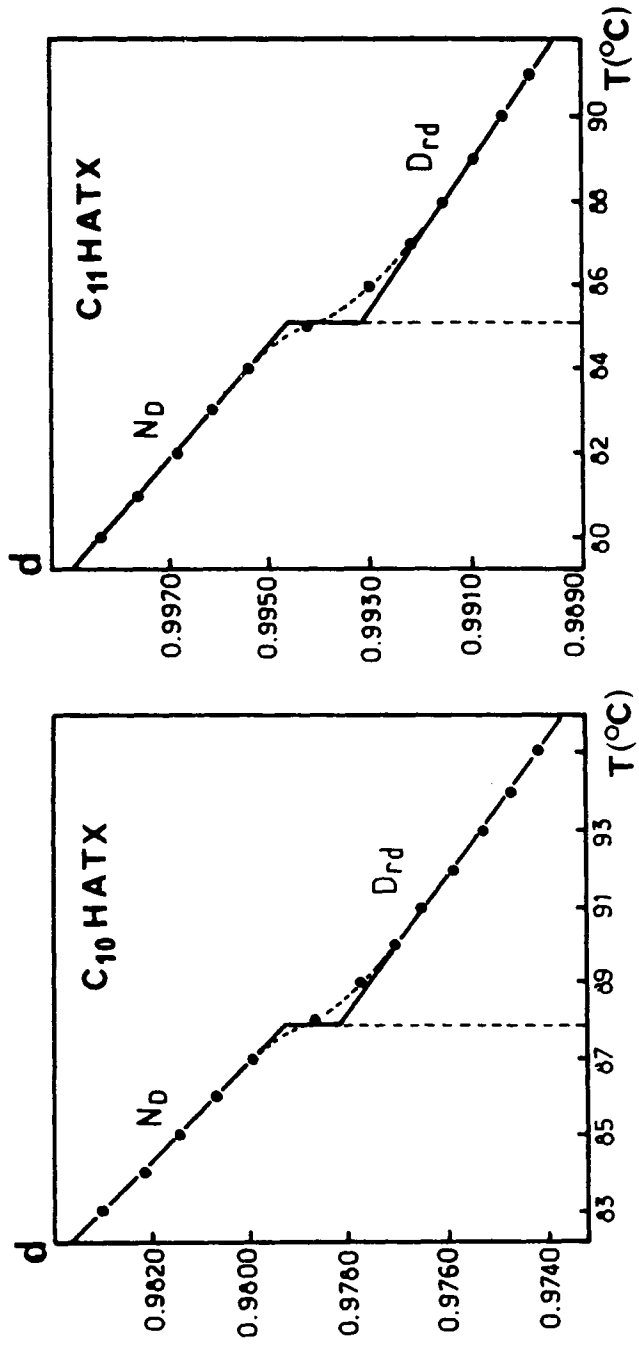

FIGURE 1 (continued)

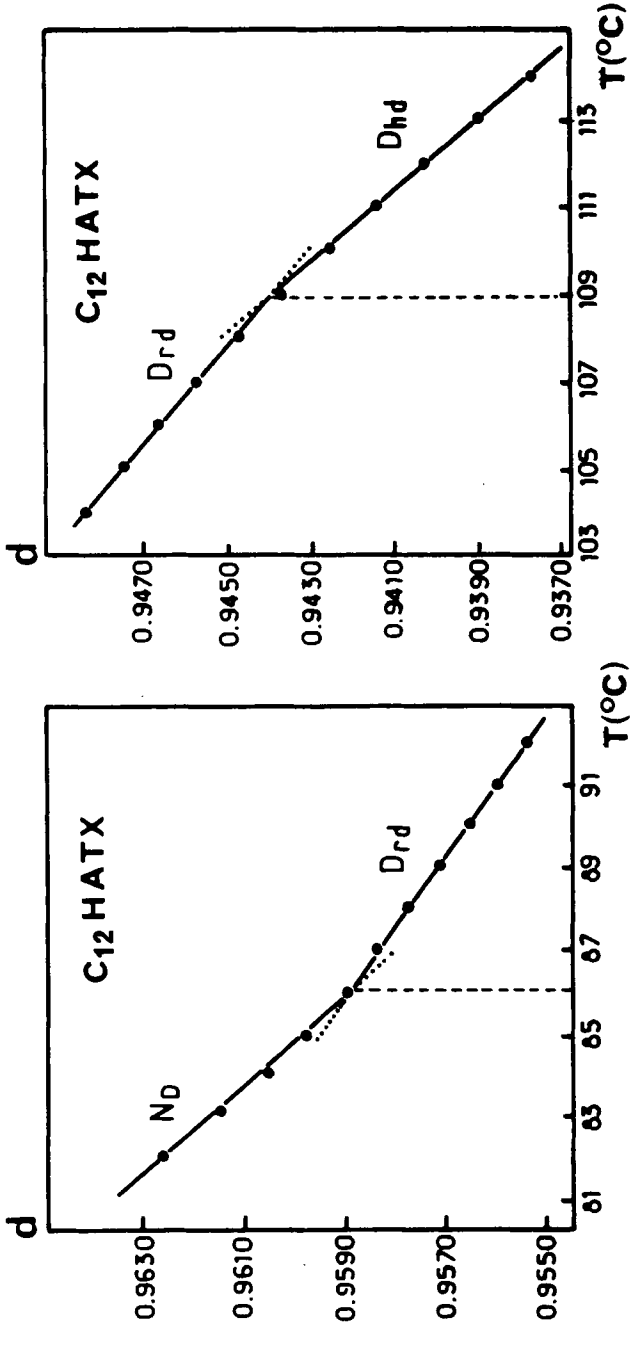

FIGURE 1 (continued)

TABLE II

Experimental data for the phases of C_n HATX:

$\left(\frac{dP}{dT}\right)_V$: Slope of the thermobarograms out of the transitions (bars·K^{-1}),

α: Thermal expansion coefficient (10^4 °C^{-1}) with the temperature T(°C) in index,

χ: isothermal compressibility coefficient (10^9 m^2·N^{-1}),

ρ: density (g·cm^{-3}), $\rho = a - bT$ with T(°C).

		K	D_h	N_D	D_{rd}	D_h
$n=8$	$\left(\frac{dP}{dT}\right)_V$	9.6		6.3	5.7	
	α			$7.1^{84.5}$	5.8^{90}	
	χ			1.1	1	
	ρ			$a=1.0767$ $b=8.2\ 10^{-4}$	$a=1.0573$ $b=6.2\ 10^{-4}$	
$n=9$	α			9.1^{81}	4.7^{89}	
	ρ			$a=1.0704$ $b=8.9\ 10^{-4}$	$a=1.0329$ $b=4.7\ 10^{-4}$	
$n=10$	$\left(\frac{dP}{dT}\right)_V$	8.8	8.0	4.6	5.4	4.7
	α			$7.4^{84.5}$	6.1^{92}	
	χ			1.6	1.1	
	ρ			$a=1.0461$ $b=7.6\ 10^{-4}$	$a=1.0274$ $b=5.61\ 10^{-4}$	

$n=11$	$\left(\frac{dP}{dT}\right)_v$	9	6.7	5	4.2	
	α			7.35[82]	5.6[90]	
	χ			1.47	1.33	
	ρ			$\begin{cases} a=1.0584 \\ b=7.5\ 10^{-4} \end{cases}$	$\begin{cases} a=1.0421 \\ b=5.8\ 10^{-4} \end{cases}$	
$n=12$	$\left(\frac{dP}{dT}\right)_v$			6.8	7.6	5.7
	α				5.7[91]	13.7[112]
	χ				0.75	2.4
	ρ			$\begin{cases} a=1.0390 \\ b=9.3\ 10^{-4} \end{cases}$	$\begin{cases} a=1.0092 \\ b=5.8\ 10^{-4} \end{cases}$	$\begin{cases} a=1.075 \\ b=1.2\ 10^{-3} \end{cases}$
$n=13$	$\left(\frac{dP}{dT}\right)_v$		5.8	4.9	5.8	

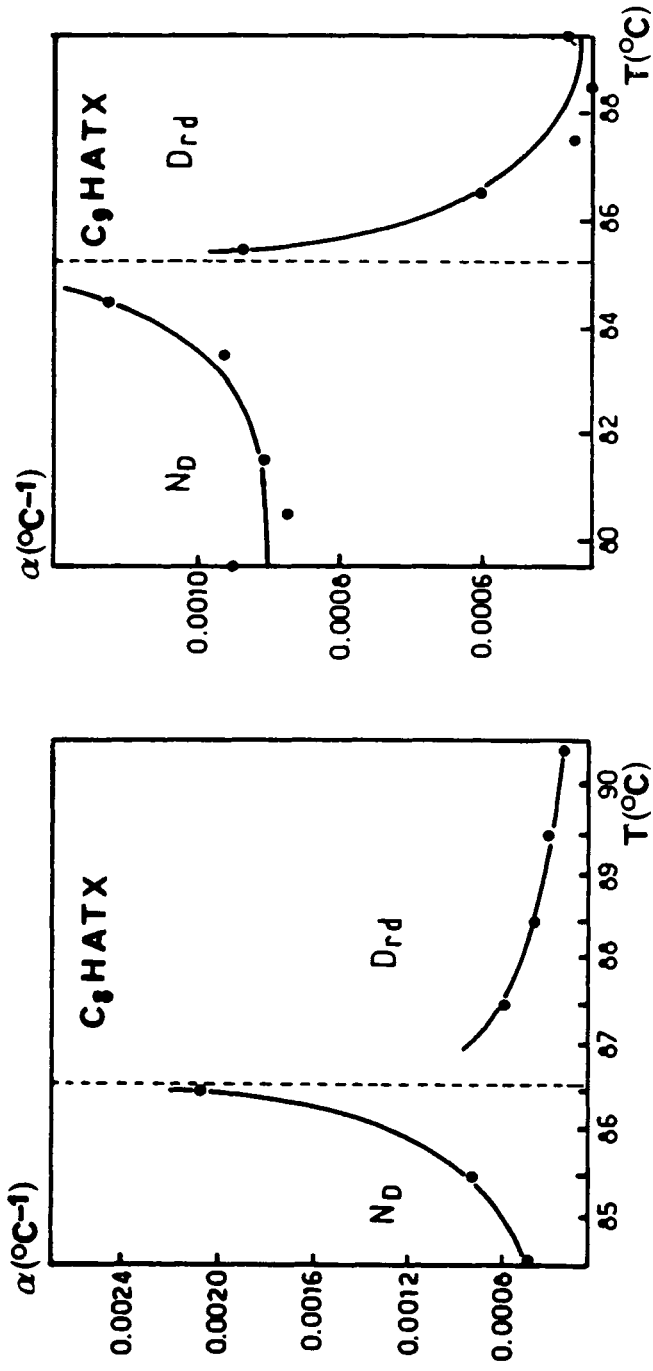

FIGURE 2 Thermal expansion coefficient versus temperature near the N_D-D_{rd} transition for Cn HATX; (a): $n = 8$, (b): $n = 9$, (c): $n = 10$, (d): $n = 11$.

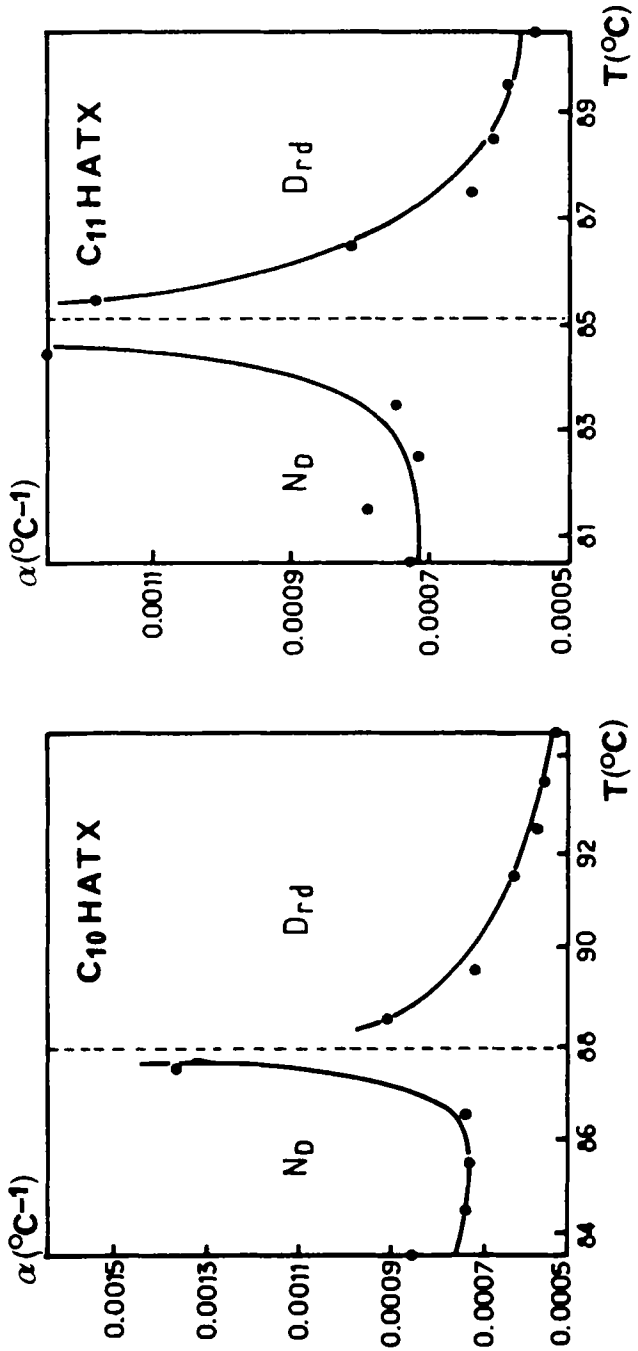

FIGURE 2 (continued)

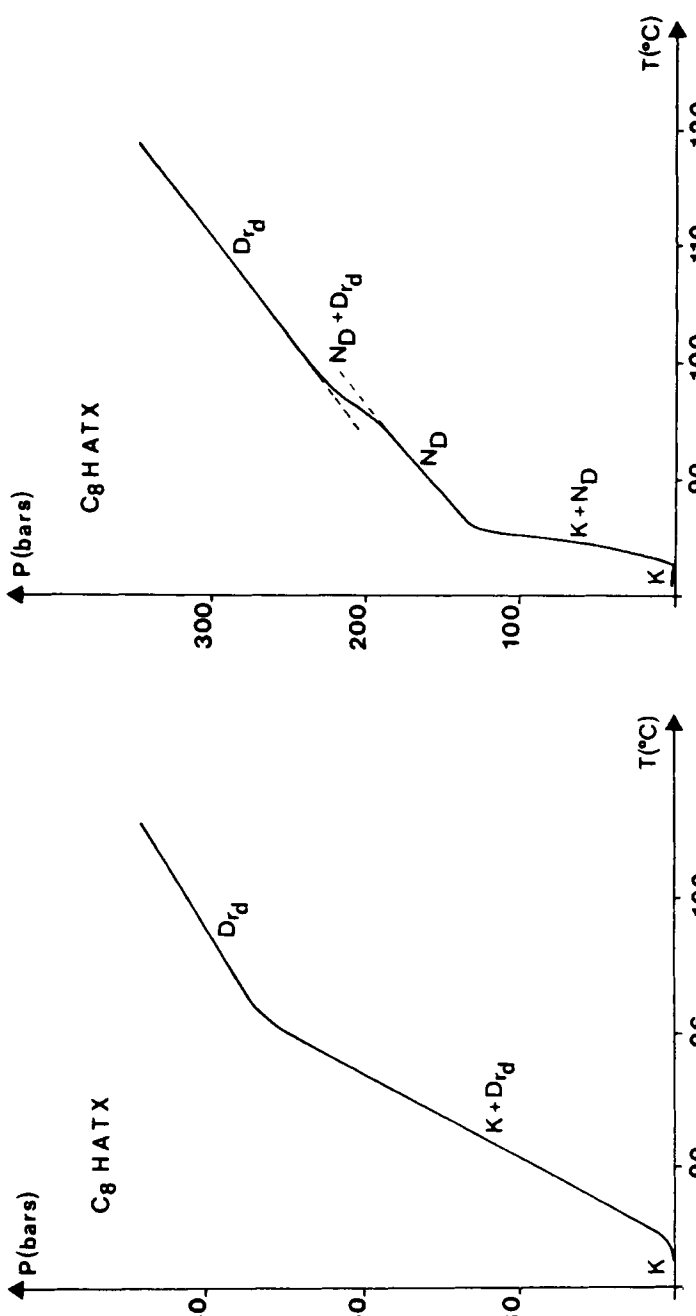

FIGURE 3 Thermobarograms obtained on heating (a) and on cooling (b) for C_8 HATX.

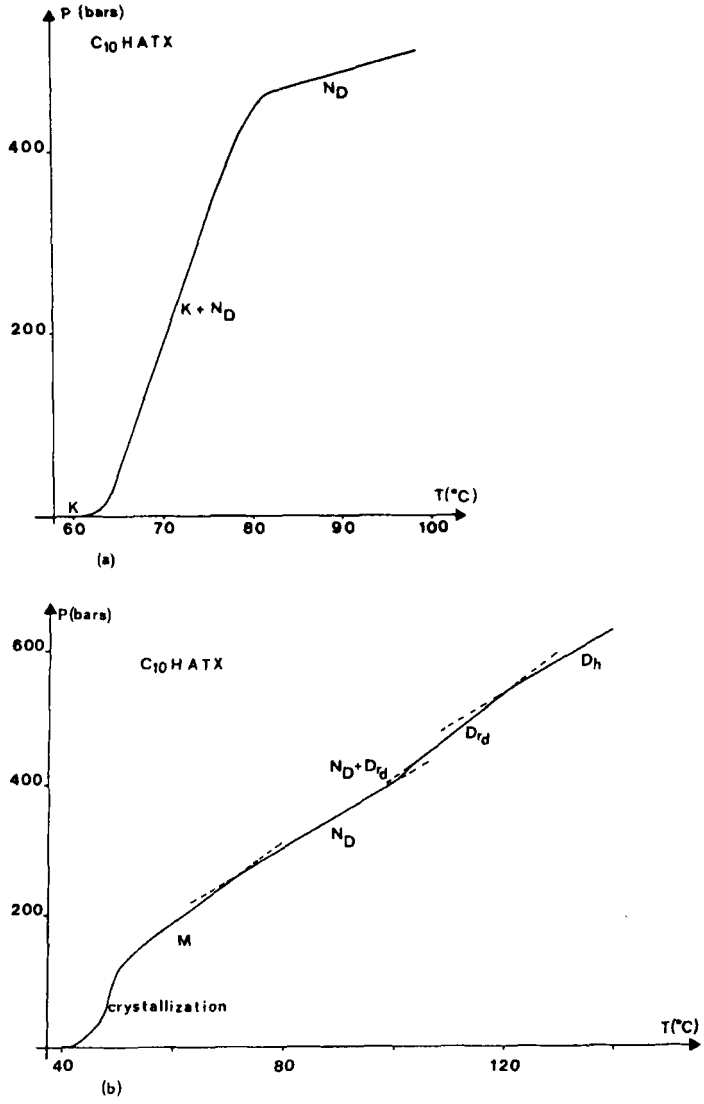

FIGURE 4 Thermobarograms obtained on heating (a) and on cooling (b) for C_{10} HATX.

sition (pressure change at 104°C under 430 bars), the D_{rd}-D_h transition (change of slope at 121°C under 512 bars), and another transition (change of slope at 72°C under 265 bars) between N_D and a phase M not observed under atmospheric pressure by microscopical observations and calorimetric measurements.[11] The thermobarograms ob-

tained on cooling for $n = 11$ and 12 have the general shape of Figure 4b and exhibit also a N_D-M transition.

For $n = 12$, from heating from room temperature, the melting (K_2-N_D) appears at 78°C under atmospheric pressure (Figure 5a). When the sample is only cooled at about 45°C, the melting (K_1-N_D) appears at 56°C (Figure 5b) under atmospheric pressure (correspond-

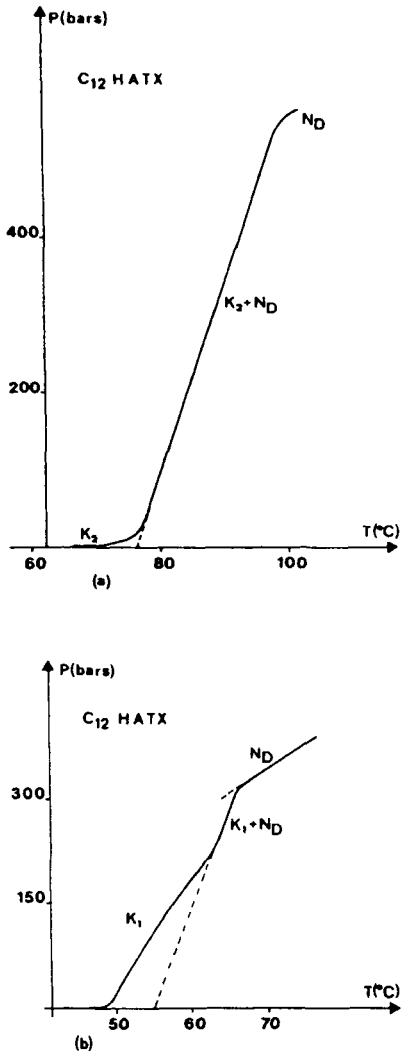

FIGURE 5 Thermobarograms obtained for the meltings at high (a) and low (b) temperatures for C_{12} HATX.

ing to the melting observed by optical microscopy.[11] By cooling K_1 under pressure a crystal-crystal transition (K_1-K_3) can be observed. That transformation can only be detected under atmospheric pressure by cooling K_1 lower than 20°C. By reheating, the K_3-K_2 transition can be detected at 50°C under atmospheric pressure.

For $n = 13$, two phase sequences are also observable for the melting (Figure 6). When the sample has been previously cooled below 10°C, the melting appears at 82°C under atmospheric pressure (Figure 6a). When the sample is only cooled at about 25°C the melting appears at 61°C under atmospheric pressure (Figure 6b). Figure 6c gives an example of thermobarogram obtained on cooling and showing the N_D-D_{rd} transition (pressure change), D_h-N_D transition (change of slope) and crystallization.

The pressure-temperature phase diagrams for the studied compounds are plotted Figure 7 to 11. Data deduced from P-T diagrams (i.e. transition temperature under atmospheric pressure, slopes of the equilibrium curves, volume changes for the transitions are reported in Table I. The slopes of thermobarograms out of the transitions are reported in Table II.

IV. DISCUSSIONS

The volume changes obtained by dilatometric studies are always larger than those obtained by thermobarometric ones. The $\Delta\mathcal{V}$ determined by density measurements include part or the whole pretransitional volume change that increases the $\Delta\mathcal{V}$ data. The slopes $(dP/dT)^E$ are determined[16-17] from the transition temperatures obtained on cooling under pressure and on heating at atmospheric pressure[5]; although the undercooling of D_{rd} is very weak (weak enthalpy change for the N_D-D_{rd} transition) that gives data a bit too large for $(dP/dT)^E$ and too small for $\Delta\mathcal{V}$. In fact the true $\Delta\mathcal{V}$ are between data obtained by both methods.

As already seen for transitions of rod-like molecules,[18] the enthalpy and volume changes (for both dilatometric and thermobarometric studies) at the N_D-D_{rd} transitions (Table I) are not dependent of the alkyl chain lengths. So the N_D-D_{rd} transition corresponds to the aromatic core reorganization: transformation of the orientational order of the cores in the N_D phase (with a rough-cast of columnar organization: cybotactic groups[19] to a two dimensional columnar order of the cores in the D_{rd} phase. The alkyl chains are, in both N_D and D_{rd} phases, in a statistical disorder very near the disorder they have in

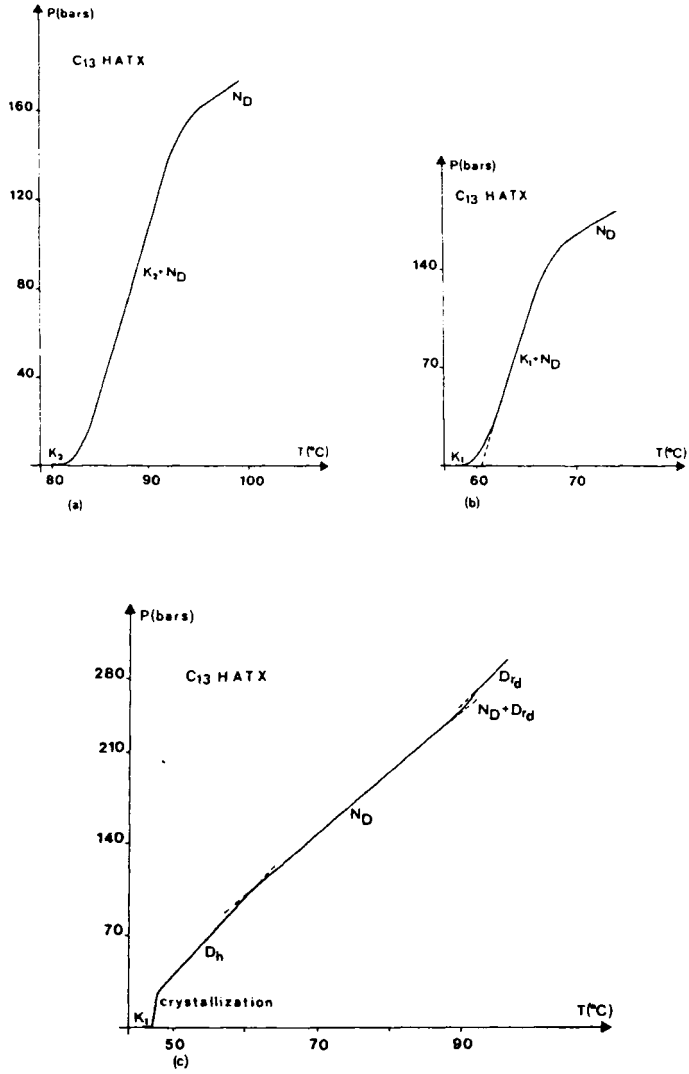

FIGURE 6 Thermobarograms obtained on heating for the meltings at high (a) and low (b) temperature and on cooling (c) for C_{13} HATX.

the isotropic state (as previously shown by spectroscopic[20] and X-ray[19] studies).

The molar volume $\mathcal{V}(n,T)$ at a temperature (T) is given, in first approximation, by the relation[21]

$$\mathcal{V}(n,T) = \mathcal{V}_{\text{core}} + 6\, n\, \mathcal{V}_{CH_2}$$

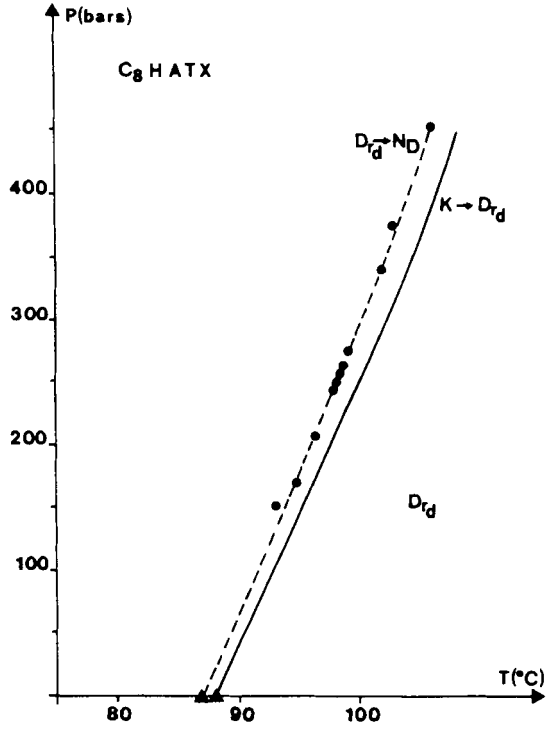

FIGURE 7 Pressure-temperature phase diagram for C_8 HATX;
▲ literature data,
● this work on cooling.

with $\mathcal{V}_{core}$ and $\mathcal{V}_{CH_2}$ the partial molar volume respectively for the aromatic core and CH_2 group and n the carbon number of the alkyl chains. From dilatometric measurements, $\mathcal{V}(n,T)$ can be plotted for n = 8 to 12 for N_D and D_{rd} respectively at 84°C and 90°C (Figure 12). The partial molar volume for the CH_2 group of both phases is 17 cm^3 $mole^{-1}$ and agrees with literature data.[21] For the aromatic core, $\mathcal{V}_{core}$ are respectively 444 $cm.^3$ $mole^{-1}$ for N_D and 454 $cm.^3$ $mole^{-1}$ for D_{rd}.

Comparison between Figure 4b (for n = 10) and Figure 6c (for n = 13) let predict the M phase is an hexagonal columnar one (D_h); the (P-T) phase diagrams (Figures 8 and 11) and the transition temperatures under atmospheric pressure (Table I) confirm the hypothesis of the existence of a D_h phase, monotropic under atmospheric pres-

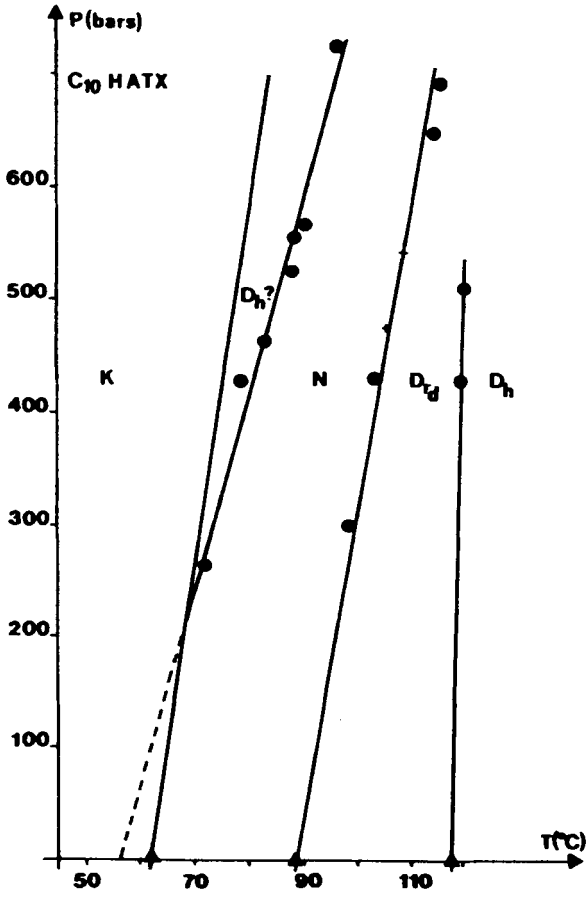

FIGURE 8 Pressure-temperature phase diagram for C_{10} HATX;
▲ literature data,
● this work (on cooling),
+ this work (on heating).

sure and enantiotropic under pressure. The same conclusions can be given for $n = 11$. Although not yet observed by optical microscopy for $n = 10$ and 11, D_h would then exist for $n \geqslant 10$. Although it has not been possible to plot the (P-T) diagram for high pressure, Figures 8 and 10b let predict triple points and perhaps maximums for the equilibrium curves between D_h and N_D or D_{rd} as it has been already seen for rod-like molecules.[22–24] To confirm these hypotheses, X ray

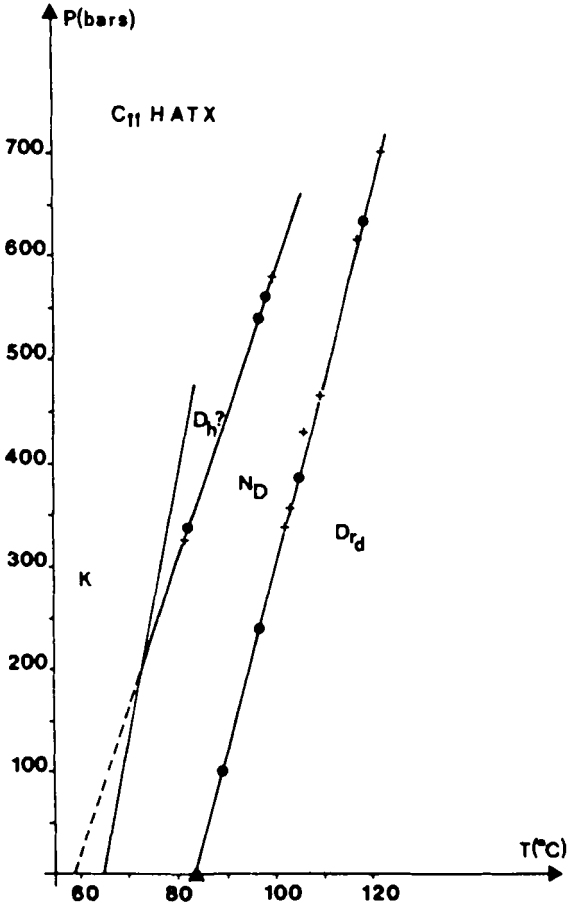

FIGURE 9 Pressure-temperature phase diagram for C_{11} HATX;
▲ literature data,
● this work (on cooling),
+ this work (on heating).

studies under pressure have to be performed. Then the phase sequence for $n = 12$ is

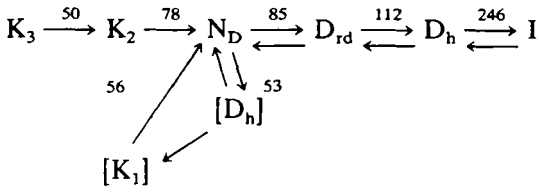

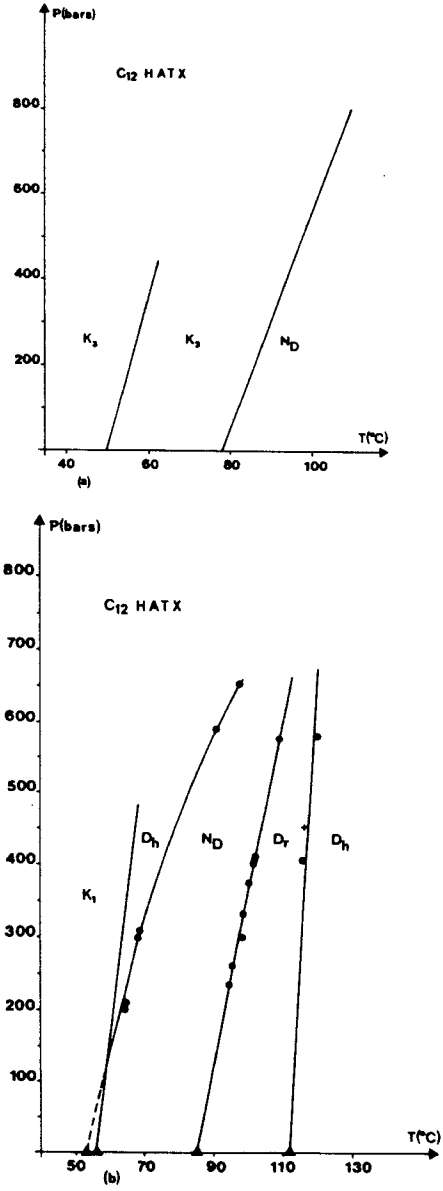

FIGURE 10 Pressure-temperature phase diagram for C_{12} HATX;
(a) for crystal-crystal transition and high temperature melting, (b) for low temperature melting and mesophase-mesophase transitions;
▲ literature data,
● this work (on cooling),
+ this work (on heating.

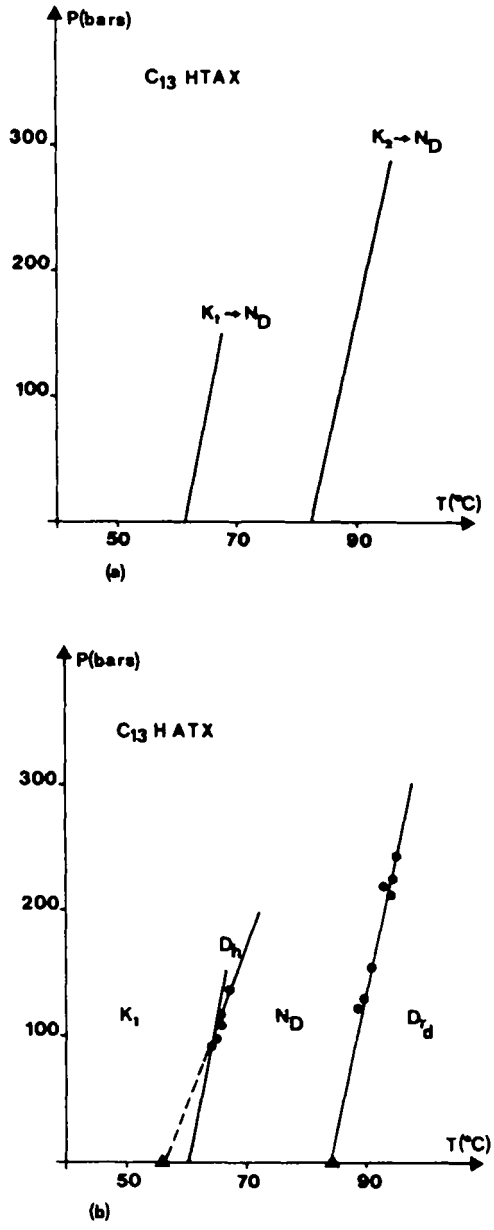

FIGURE 11 Pressure-temperature phase diagram for C_{13} HATX; (a) for the meltings, (b) for the low temperature melting and mesophase-mesophase transitions;
▲ literature data,
● this work (on cooling),

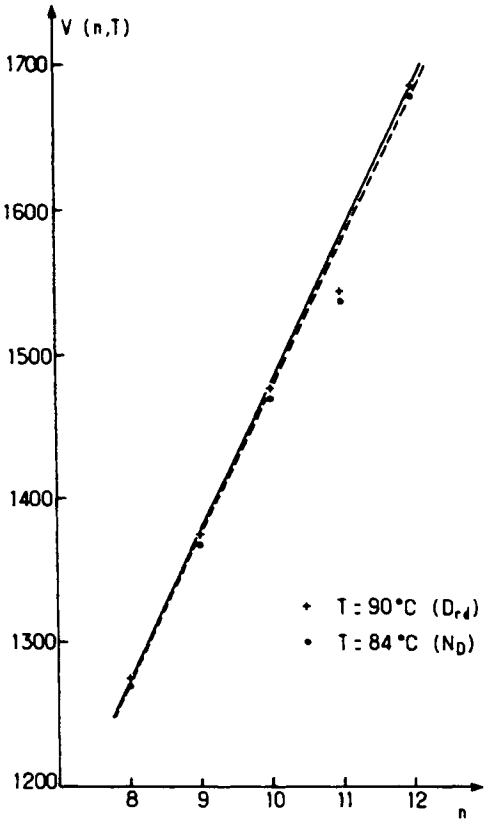

FIGURE 12 Molar volume $\mathcal{V}(n,T)$ versus the carbon number of the alkyl chains for the N_D (at 84°C) and D_{rd} (at 90°C) phases of C_n HATX.

Relating to the crystalline phases a similar sequence has already been detected for disc-like mesogens by thermal analysis under atmospheric pressure for (−) and (+) 2,3,6,7,10,11-hexa-[S-(3-methyl)-*n* nonanoyloxytriphenylene.[25] The phase sequence for $n = 13$ is

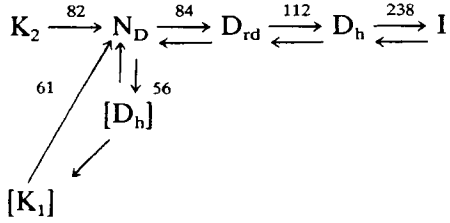

The K_1 phases previously observed by microscopical and calorimetric studies[11] are in fact monotropic phases.

Changes for the ratio α/χ (thermal expansion/isothermal compressibility coefficients) for pressure lower than 1.kbar are weak.[15] So, orders of magnitude for χ can be calculated for α (taken under atmospheric pressure) and the slopes ($(dP/dT)_V = \alpha/\chi$) of the thermobarograms out of the transitions (taken for pressures between .2 and .4 kbars); they are reported in Table II. Such data are the first ones for disc-like mesogens.

CONCLUSION

Dilatometric and thermobarometric measurements have been performed on some members of the series of truxene derivatives Cn HATX. Volume changes are determined for most of the transitions; data obtained by both methods for the N_D-D_{rd} transition have been compared. It has been confirmed that the N_D-D_{rd} transition corresponds to the transformation of the orientational order of the aromatic cores in N_D to a two-dimensional columnar order of the cores in D_{rd}. The partial molar volumes at a given temperature for both phases has been determined for the aromatic cores and CH_2 groups. Data for the thermal expansion and isothermal compressibility coefficients have been calculated for the N_D and D_{rd} phases. Last P-T phase diagrams have been plotted; a monotropic phase is observed under atmospheric pressure at lower temperature that N_D for n = 10 and 11 and it seems it's a D_h phase. These diagrams let predict a maximum for the equilibrium curve between D_h and N_D or D_{rd} for $n \simeq 10$ and 12.

Remark

Confirmations for the existence of the reentrant monotropic D_h phase under atmospheric pressure for C_{10} and C_{11} HATX and for the complex phase sequence for C_{12} HATX has just been confirmed whereas this paper was in press. Details will be published in C. R. Acad. Sc. Paris II by J. M. Buisine and M. Domon.

References

1. T. H. Smith and G. R. Van Hecke, *Mol. Cryst. Liq. Cryst.*, **68**, 23 (1981).
2. S. Chandrasekhar, B. K. Sadashiva, K. A. Suresh, N. V. Madhusudana, S. Kumar, R. Shashidhar and G. Venkatesh, *J. de Phys.*, **40**, C3, 120 (1979).

3. H. Gasparoux, M. F. Achard, F. Hardouin and G. Sigaud, *C.R. Acad. Sci.*, Paris II, **293**, 1029 (1981).
4. V. N. Raja, R. Shashidhar, S. Chandrasekhar, R. E. Boehm and D. E. Martire, Pramana, **25**L, 119 (1985).
5. J. M. Buisine, J. Malthete, C. Destrade and Nguyen Huu Tinh, *Physica B*, **139** and **140**B, 631 (1986).
6. C. Destrade, J. Malthete, Nguyen Huu Tinh and H. Gasparoux, *Phys. Lett.*, **79A**, 189 (1980).
7. C. Destrade, H. Gasparoux, A. Babeau, Nguyen Huu Tinh and J. Malthete, *Mol. Cryst. Liq. Cryst.*, **67**, 37 (1981).
8. Nguyen Huu Tinh, R. Cayuela, C. Destrade and J. Malthete, *Mol. Cryst. Liq. Cryst.*, **122**, 141 (1985).
9. Nguyen Huu Tinh, J. Malthete and C. Destrade, *Mol. Cryst. Liq. Cryst. Lett.*, **64**, 291 (1981).
10. Nguyen Huu Tinh, J. Malthete and C. Destrade, *J. de Phys.*, **18**, L 417 (1981).
11. Nguyen Huu Tinh, P. Foucher, C. Destrade, A. M. Levelut and J. Malthete, *Mol. Cryst. Liq. Cryst.*, **111**, 277 (1984).
12. D. Armitage and F. P. Price, *J. of Chem. Phys.*, **66**, 3414 (1977).
13. D. Armitage and F. P. Price, *Mol. Cryst. Liq. Cryst.*, **38**, 229 (1977).
14. J. M. Buisine and B. Soulestin, (to be published).
15. J. M. Buisine, B. Soulestin and J. Billard, *Mol. Cryst. Liq. Cryst.*, **91**, 115 (1983).
16. J. M. Buisine, B. Soulestin and J. Billard, *Mol. Cryst. Liq. Cryst.*, **97** 397 (1983).
17. J. M. Buisine, *Mol. Cryst. Liq. Cryst.*, **109**, 143 (1984).
18. P. Seurin, D. Guillon and A. Skoulios, *Mol. Cryst. Liq. Cryst.*, **65**, 85 (1983).
19. A. M. Levelut, *J. Chim. Phys.*, **80**, 150 (1983).
20. M. Kardan, B. B. Reinhold, Shaw Ling Hsu, R. Tarur and A. Lill, *Macromolecules*, **19**, 616 (1986).
    M. Rey-Lafon, C. Destrade and Azzedine Tazi Hemida, *Mol. Cryst. Liq. Cryst.* (to appear).
21. D. Guillon and A. Skoulios, *J. de Phys.*, **37**, 797 (1976).
22. P. E. Cladis, R. K. Bogardus, W. B. Daniels and G. N. Taylor, *Phys. Rev. Lett.*, **39**, 720 (1977).
23. L. Liebert and W. B. Daniels, *J. de Phys.*, L **38**, 333 (1977).
24. A. N. Kalkura, R. Shashidhar and N. Subramanya Raj Urs, *J. de Phys.*, **44**, 51 (1983).
25. F. Mbama and J. M. Buisine, unpublished results.